

Research Article

Formation of Large Amplitude Solitons and Small Amplitude Double Layers in Two-temperature Non-isothermal Electron Plasma

Sankar Chattopadhyay* 

Department of Mathematics, Sishu Bikash Academy, Kolkata, India

Abstract

Propagation of large amplitude ion-acoustic solitary waves and small amplitude double layers have been investigated in a two-temperature non-isothermal electron plasma consisting of warm positive ions, warm negative ions and warm positrons by Sagdeev pseudopotential method (SPM). Small amplitude double layer solution (ϕ_{DL}) is also discussed theoretically in this paper for further investigation. Fully non-linear large amplitude compressive solitary waves and small amplitude compressive double layers are presented graphically by the corresponding figures 1 – 14 under the variation of different values of the mass ratios (Q) of negative to positive ions, phase velocities (V) of solitary waves, negative ion concentrations (n_{j0}), positron densities (χ) and temperature ratios (σ_p) of electrons (T_e) and positrons (T_p). Consequently this large amplitude electrostatic solitary waves and small amplitude electrostatic double layers in complex plasmas have broad applications in space plasma Physics, Astrophysics, Fusion technology, Plasma – based devices and Fundamental wave research, offering tools for exploring wave-particle interactions, stability and energy transfer in multi-species plasmas.

Keywords

Solitary Waves, Two-Temperature Non-Isothermal Electron Plasma, Double Layers, Double Layer Width and Amplitude, Double Layer Velocity

1. Introduction

Propagation of large amplitude ion-acoustic solitary waves and small amplitude ion-acoustic double layers have been investigated theoretically in a plasma consisting of warm positive ions, warm negative ions and warm positrons along with isothermal, non-isothermal and non-thermal electrons by many authors [1-11]. A large number of physicists [12-16] investigated various types of solitary waves for warm or cold ions with magnetized or unmagnetized plasmas in presence of two-temperature or single-temperature non-isothermal electrons.

Solitary waves became more interesting when negative ions are found in space plasmas. This negative ions are observed in D and F regions of the earth's ionosphere, in Saturn's moons and in Halley's cometarycomae. Wong, Mamas and Arnush [17] discussed a method for producing plasmas with total replacement of electrons by negative ions. On the other hand, non-isothermal electrons [18-20] give rise many interesting results in the propagation of waves. It is also found that two-temperature Maxwellian distribution of electrons [21, 22] presents a better result

*Corresponding author: sankardjln@gmail.com (Sankar Chattopadhyay)

Received: 23 October 2024; **Accepted:** 15 November 2024; **Published:** 30 December 2024



Copyright: © The Author(s), 2024. Published by Science Publishing Group. This is an **Open Access** article, distributed under the terms of the Creative Commons Attribution 4.0 License (<http://creativecommons.org/licenses/by/4.0/>), which permits unrestricted use, distribution and reproduction in any medium, provided the original work is properly cited.

nearer to the experimental data for the formation of solitons and double layers. Ion-acoustic double layers have been extensively studied theoretically [23-25] as well as experimentally [26-28] by many plasma physicists. Das et al [29], Watanabe [30] and Tagare [31] investigated theoretically and Cooney et al [32] investigated experimentally the ion-acoustic solitary waves in a multispecies plasma. Mishra et al [33] studied the ion-acoustic compressive and rarefactive double layers in a warm plasma by reductive perturbation method. Consequently Merlino and Loomis [34] discussed strong double layers experimentally for (Ar⁺, SF₆⁻) plasma. Chattopadhyay et al [35, 36] also studied the effect of negative ions on the formation of ion-acoustic solitons for cold and warm ions in relativistic and in non-relativistic plasmas by Sagdeev pseudopotential method [37]. In magnetized plasma with or without negative ions, Ghosh et al and Das et al [38, 39] studied the ion-acoustic solitary waves by a new analytical method and reductive perturbation method. In the auroral and magnetospheric plasmas, ion-acoustic double layers have been observed for two-electron species [40, 41]. It is therefore interesting to investigate the ion-acoustic double layers in a plasma where negative ions and two-temperature electron distributions present simultaneously. Again, the electrostatic waves show a significant change and behave differently when positrons are introduced in addition to three component plasmas. Popel et al [42] found that the amplitude of ion-acoustic solitary waves could be considerably reduced when hot positrons were present. We are now wishing to study the ion-acoustic solitary waves and double layers when positrons are included in our system for two-temperature non-isothermal electron plasmas. In presence of warm negative ions, warm positive ions and warm positrons, the present author in recent year [4, 18] discussed critically the solitary waves and small amplitude double layers under the variation of different plasma parameters for two-temperature non-isothermal electron plasmas by SPM.

The aim of this paper is to discuss the large amplitude ion-acoustic compressive solitary waves and small amplitude ion-acoustic compressive double layers in a multicomponent plasma consisting of warm positive ions, warm negative ions, warm positrons and two-temperature non-isothermal electrons by SPM. By taking some plasmas containing ion species (Ar⁺, SF₆⁻), (H⁺, O₂⁻) and (He⁺, O⁻), the profiles of Sagdeev potential function ψ(φ) for large amplitude ion-acoustic compressive solitons and small amplitude compressive double layers are drawn under the variation of negative to positive ion mass ratios (Q), phase velocities (V) of solitary waves, negative ion concentrations (n_{jo}), positron density (χ)

and temperature ratios (σ_p) of electrons (T_e) and positrons (T_p).

The plan of this paper is arranged in the following ways:

The basic set of normalized fluid equations for positive ions, negative ions along with Poisson's equations, concentrations of two-temperature non-isothermal electrons and warm isothermal positrons are given in Sec.2. The Sagdeev potential function ψ(φ) for soliton is given in this section. By using the double layer conditions, the profiles of Sagdeev potential function ψ(φ) for small amplitude compressive double layers and double layer solutions (φ_{DL}) are stated clearly in this part. In sec.3, the entire problem is discussed critically under the variation of different plasma parameters. Concluding remarks are given in sec.4.

2. Formulations

In presence of warm positrons, the set of normalized fluid equations for a collisionless, unmagnetized, non-relativistic plasma containing warm positive ions, warm negative ions and two-temperature non-isothermal electrons along with charge neutrality condition are given in the following ways:

$$\frac{\partial n_i}{\partial t} + \frac{\partial}{\partial x} (n_i u_i) = 0 \tag{1}$$

$$\frac{\partial u_i}{\partial t} + u_i \frac{\partial u_i}{\partial x} + \frac{\sigma_i}{n_i} \frac{\partial p_i}{\partial x} = -\frac{\partial \phi}{\partial x} \tag{2}$$

$$\frac{\partial p_i}{\partial t} + u_i \frac{\partial p_i}{\partial x} + 3 p_i \frac{\partial u_i}{\partial x} = 0 \tag{3}$$

$$\frac{\partial n_j}{\partial t} + \frac{\partial}{\partial x} (n_j u_j) = 0 \tag{4}$$

$$\frac{\partial u_j}{\partial t} + u_j \frac{\partial u_j}{\partial x} + \frac{\sigma_j}{Q n_j} \frac{\partial p_j}{\partial x} = \frac{z}{Q} \frac{\partial \phi}{\partial x} \tag{5}$$

$$\frac{\partial p_j}{\partial t} + u_j \frac{\partial p_j}{\partial x} + 3 p_j \frac{\partial u_j}{\partial x} = 0 \tag{6}$$

$$\frac{\partial^2 \phi}{\partial x^2} = n_e - n_i + Z n_j - n_p \tag{7}$$

Charge neutrality condition is

$$1 + Z n_{jo} = n_{io} + \chi \tag{8}$$

where

$$n_e = 1 + \phi - \frac{4}{3} \frac{\left(\mu b_l + \nu b_h \beta_l^2 \right)^{\frac{3}{2}}}{(\mu + \nu \beta_l)^{\frac{3}{2}}} \phi^{\frac{3}{2}} + \frac{1}{2} \frac{(\mu + \nu \beta_l^2)}{(\mu + \nu \beta_l)^2} \phi^2 - \frac{8}{15} \frac{\left(\mu b_l^{(1)} + \nu b_h^{(1)} \beta_l^2 \right)^{\frac{5}{2}}}{(\mu + \nu \beta_l)^{\frac{5}{2}}} \phi^{\frac{5}{2}} + \frac{1}{6} \frac{(\mu + \nu \beta_l^3)}{(\mu + \nu \beta_l)^3} \phi^3 - \dots \tag{9}$$

$$n_p = \chi e^{-\sigma_p \phi} \tag{10}$$

$$b_l = \frac{1 - \beta_l}{\sqrt{\pi}}, \quad b_h = \frac{1 - \beta_h}{\sqrt{\pi}}, \quad b_l^{(1)} = \frac{1 - \beta_l^2}{\sqrt{\pi}}, \quad b_h^{(1)} = \frac{1 - \beta_h^2}{\sqrt{\pi}}, \quad \beta_1 = \frac{T_{ehf}}{T_{ehf}}$$

$$\beta_l = \frac{T_{el,f}}{T_{el,t}}, \beta_h = \frac{T_{eh,f}}{T_{eh,t}}, \mu + \nu = 1$$

$$\sigma_p = \frac{T_{eff}}{T_p}, \sigma_i = \frac{T_i}{T_{eff}}, \sigma_j = \frac{T_j}{T_{eff}}, T_{eff} = \frac{T_{el}T_{eh}}{\mu T_{eh} + \nu T_{el}}$$

For non-isothermal plasma $0 < b_l$ or $b_h < \frac{1}{\sqrt{\pi}}$ and $0 < b_l^{(1)}$ or $b_h^{(1)} < \frac{1}{\sqrt{\pi}}$

In this case, $T_{el,f}$ = temperature of free electrons in low temperature, $T_{eh,f}$ = temperature of free electrons in high temperature, $T_{el,t}$ = temperature of trapped electrons in low temperature, $T_{eh,t}$ = temperature of trapped electrons in high temperature, T_{eff} = effective temperature of electrons, T_p = temperature of positrons, T_i = temperature of positive ions, T_j = temperature of negative ions.

The concerned plasma parameters $n_i, n_j, n_e, n_p, u_i, u_j, p_i, p_j, \sigma_i, \sigma_j, \phi, Z, Q, \chi, \sigma_p, x, t, \mu, \nu, \beta_1, \beta_l, \beta_h, b_l, b_h, b_l^{(1)}$ and $b_h^{(1)}$ in equations (1) to (10) are respectively the density of positive ions, negative ions, electrons and positrons, the velocity of positive ion and negative ions, the pressure of positive ions and negative ions, the temperature of positive ions and negative ions, the

electrostatic potential, charge of ions, mass ratio of negative to positive ions, density of positron at $\phi = 0$, temperature ratio of electrons and positrons, distance, time, the unperturbed number density of low temperature and high temperature electrons, the temperature ratio of free electrons in low and high temperatures, the temperature ratio of free and trapped electrons in low temperature, the temperature ratio of free and trapped electrons in high temperature and the normally used conventional non-isothermal parameters related with β_l and β_h .

In this paper the boundary conditions for our systems are

$$n_i \rightarrow n_{i0}, n_j \rightarrow n_{j0}, u_i \rightarrow u_{i0}, u_j \rightarrow u_{j0}, p_i \rightarrow 1, p_j \rightarrow 1, n_e \rightarrow 1, n_p \rightarrow \chi \text{ and } \phi \rightarrow 0 \text{ at } |x| \rightarrow \infty$$

In equations (1) to (7), the Galilean transformation $\eta = x - Vt$ is used where V is the velocity of the solitary waves.

Following Chattopadhyay [4], the expression for Sagdeev pseudopotential function $\psi(\phi)$ for two-temperature non-isothermal electron plasmas with warm positive ions, warm negative ions and warm positrons, is obtained as

$$\begin{aligned} \psi(\phi) = & \left[-\phi - \frac{1}{2}\phi^2 + \frac{8}{15} \frac{\mu b_l + \nu b_h \beta_1^{\frac{3}{2}}}{(\mu + \nu \beta_1)^{\frac{3}{2}}} \phi^{\frac{5}{2}} - \frac{1}{6} \frac{\mu + \nu \beta_1^2}{(\mu + \nu \beta_1)^2} \phi^3 + \frac{16}{105} \frac{\mu b_l^{(1)} + \nu b_h^{(1)} \beta_1^{\frac{5}{2}}}{(\mu + \nu \beta_1)^{\frac{5}{2}}} \phi^{\frac{7}{2}} - \frac{1}{24} \frac{\mu + \nu \beta_1^3}{(\mu + \nu \beta_1)^3} \phi^4 + \dots \right] \\ & + \frac{1}{6} \sqrt{\frac{n_{i0}^3}{3\sigma_i}} \left[\left\{ \left(V - u_{i0} - \sqrt{\frac{3\sigma_i}{n_{i0}}} \right)^2 - 2\phi \right\}^{\frac{3}{2}} - \left\{ \left(V - u_{i0} + \sqrt{\frac{3\sigma_i}{n_{i0}}} \right)^2 - 2\phi \right\}^{\frac{3}{2}} \right. \\ & \left. + \left(V - u_{i0} + \sqrt{\frac{3\sigma_i}{n_{i0}}} \right)^3 - \left(V - u_{i0} - \sqrt{\frac{3\sigma_i}{n_{i0}}} \right)^3 \right] \\ & + \frac{1}{6} \sqrt{\frac{Q^3 n_{j0}^3}{3\sigma_j}} \left[\left\{ \left(V - u_{j0} - \sqrt{\frac{3\sigma_j}{Q n_{j0}}} \right)^2 + \frac{2Z\phi}{Q} \right\}^{\frac{3}{2}} - \left\{ \left(V - u_{j0} + \sqrt{\frac{3\sigma_j}{Q n_{j0}}} \right)^2 + \frac{2Z\phi}{Q} \right\}^{\frac{3}{2}} \right. \\ & \left. + \left(V - u_{j0} + \sqrt{\frac{3\sigma_j}{Q n_{j0}}} \right)^3 - \left(V - u_{j0} - \sqrt{\frac{3\sigma_j}{Q n_{j0}}} \right)^3 \right] + \frac{\chi}{\sigma_p} (1 - e^{-\sigma_p \phi}) \end{aligned} \tag{11}$$

Where

$$n_i = \frac{1}{2} \sqrt{\frac{n_{i0}^3}{3\sigma_i}} \left[\sqrt{\left(V - u_{i0} + \sqrt{\frac{3\sigma_i}{n_{i0}}} \right)^2 - 2\phi} - \sqrt{\left(V - u_{i0} - \sqrt{\frac{3\sigma_i}{n_{i0}}} \right)^2 - 2\phi} \right] \tag{12}$$

$$n_j = \frac{1}{2} \sqrt{\frac{Q n_{j0}^3}{3\sigma_j}} \left[\sqrt{\left(V - u_{j0} + \sqrt{\frac{3\sigma_j}{Q n_{j0}}} \right)^2 + \frac{2Z\phi}{Q}} - \sqrt{\left(V - u_{j0} - \sqrt{\frac{3\sigma_j}{Q n_{j0}}} \right)^2 + \frac{2Z\phi}{Q}} \right] \tag{13}$$

The requirements to yield soliton solutions from Sagdeev potential function $\psi(\phi)$ are

- (i) $\psi(\phi) = \frac{\partial \psi(\phi)}{\partial \phi} = 0$ at $\phi = 0$.
- (ii) $\frac{\partial^2 \psi(\phi)}{\partial \phi^2} \leq 0$ at $\phi = 0$.
- (iii) $\psi(\phi) = 0$ at $\phi = \phi_m$ and $\psi(\phi) < 0$ for $0 < \phi < \phi_m$.
- (iv) $\frac{\partial^3 \psi(\phi)}{\partial \phi^3} > 0$ at $\phi = 0$ for positive (compressive) potential

solitons.

- (v) $\frac{\partial \psi(\phi)}{\partial \phi} > 0$ at $\phi = \phi_m$ for positive (compressive) potential solitons.

And the restriction on ϕ is

$$-\frac{Q}{2Z} \left(V - u_{j0} - \sqrt{\frac{3\sigma_j}{Q n_{j0}}} \right)^2 < \phi < \frac{1}{2} \left(V - u_{i0} - \sqrt{\frac{3\sigma_i}{n_{i0}}} \right)^2 \tag{14}$$

Now by using the Galelian transformation and the necessary boundary conditions, it is found from equations (7), (9), (10), (11), (12) and (13) after expansion of $\psi(\phi)$ in power series

$$\frac{d^2\phi}{d\eta^2} = H_1\phi - H_2\phi^2 + H_3\phi^3 - H_4\phi^4 + H_5\phi^5 - \dots = -\frac{\partial\psi}{\partial\phi} \tag{15}$$

And

$$\psi(\phi) = -\frac{1}{2}H_1\phi^2 + \frac{2}{5}H_2\phi^{\frac{5}{2}} - \frac{1}{3}H_3\phi^3 + \frac{2}{7}H_4\phi^{\frac{7}{2}} - \frac{1}{4}H_5\phi^4 \tag{16}$$

Where

$$H_1 = \left[1 - n_{i0} \left\{ (V - u_{i0})^2 - \frac{3\sigma_i}{n_{i0}} \right\}^{-1} - Z^2 n_{j0} \left\{ Q(V - u_{j0})^2 - \frac{3\sigma_j}{n_{j0}} \right\}^{-1} + \chi\sigma_p \right]$$

$$H_2 = \frac{4}{3} \frac{(\mu b_l + \nu b_h \beta_1^{\frac{3}{2}})}{(\mu + \nu \beta_1)^{\frac{3}{2}}}$$

$$H_3 = \frac{1}{2} \left[\frac{\mu + \nu \beta_1^2}{(\mu + \nu \beta_1)^2} - \frac{n_{i0}^{\frac{3}{2}}}{2\sqrt{3}\sigma_i} \left\{ (V - u_{i0} - \sqrt{\frac{3\sigma_i}{n_{i0}}})^{-3} - (V - u_{i0} + \sqrt{\frac{3\sigma_i}{n_{i0}}})^{-3} \right\} \right. \\ \left. + \frac{Z^3 n_{j0}^{\frac{3}{2}}}{2Q\sqrt{3}\sigma_j} \left\{ (V - u_{j0} - \sqrt{\frac{3\sigma_j}{Qn_{j0}}})^{-3} - (V - u_{j0} + \sqrt{\frac{3\sigma_j}{Qn_{j0}}})^{-3} \right\} - \chi\sigma_p^2 \right]$$

$$H_4 = \frac{8}{15} \frac{(\mu b_l^{(1)} + \nu b_h^{(1)} \beta_1^{\frac{5}{2}})}{(\mu + \nu \beta_1)^{\frac{5}{2}}}$$

$$H_5 = \frac{1}{2} \left[\frac{1}{3} \frac{\mu + \nu \beta_1^3}{(\mu + \nu \beta_1)^3} - \frac{n_{i0}^{\frac{3}{2}}}{2\sqrt{3}\sigma_i} \left\{ (V - u_{i0} - \sqrt{\frac{3\sigma_i}{n_{i0}}})^{-5} - (V - u_{i0} + \sqrt{\frac{3\sigma_i}{n_{i0}}})^{-5} \right\} \right. \\ \left. + \frac{Z^4 n_{j0}^{\frac{3}{2}}}{2Q^2\sqrt{3}\sigma_j} \left\{ (V - u_{j0} + \sqrt{\frac{3\sigma_j}{Qn_{j0}}})^{-5} - (V - u_{j0} - \sqrt{\frac{3\sigma_j}{Qn_{j0}}})^{-5} \right\} + \frac{\chi\sigma_p^3}{3} \right] \tag{17}$$

In order to get the small amplitude double layer profiles from Sagdeev potential function $\psi(\phi)$ and small amplitude double layer solutions (ϕ_{DL}), the Sagdeev potential $\psi(\phi)$ should satisfy the following conditions [4]:

$$\psi(\phi) = 0 \text{ at } \phi = 0 \text{ and } \phi = \phi_{dl}$$

$$\frac{\partial\psi}{\partial\phi} = 0 \text{ at } \phi = 0 \text{ and } \phi = \phi_{dl}$$

$$\frac{\partial^2\psi}{\partial\phi^2} < 0 \text{ at } \phi = 0 \text{ and } \phi = \phi_{dl}$$

$$\psi(\phi) < 0 \text{ for } 0 < \phi < \phi_{dl} \text{ and } \phi > \phi_{dl} \tag{18}$$

where $\phi_{dl} (> 0)$ is some extreme value of the electrostatic potential ϕ at which double layer is produced.

Now taking terms upto ϕ^2 in equation (15) and ϕ^3 in equation (16), we get finally after using the above boundary conditions for double layers as

$$H_1 = \frac{2}{3}H_3\phi_{dl} \text{ and } H_2 = \frac{5}{3}H_3\phi_{dl}^{\frac{1}{2}} \tag{19}$$

In terms of H_3 we get finally from equations (15) and (16) after simplification as

$$\psi(\phi) = -\frac{1}{3}H_3\phi^2(\sqrt{\phi} - \sqrt{\phi_{dl}})^2 \tag{20}$$

$$\frac{\partial\psi(\phi)}{\partial\phi} = -\frac{1}{3}H_3\phi(\sqrt{\phi} - \sqrt{\phi_{dl}})(3\sqrt{\phi} - 2\sqrt{\phi_{dl}}) \tag{21}$$

$$\phi_{DL} = \frac{1}{4}\phi_{dl} \left[1 - \tanh\left(\sqrt{\frac{H_3\phi_{dl}}{24}} \cdot \eta\right) \right]^2 \tag{22}$$

Where $H_3 > 0$ represents the stable structure of double layer. Equations (20) to (22) give us the first order double layer profile and first order double layer solution.

3. Results and Discussions

In this section, the profiles of Sagdeev potential function $\psi(\phi)$ against electrostatic potential ϕ for large amplitude solitons and small amplitude double layers are drawn under the variation of different plasma parameters.

In **Figure 1**, the profiles of Sagdeev potential function $\psi(\phi)$ against electrostatic potential ϕ for large amplitude solitary waves are drawn under the variation of the mass ratios (Q) of negative (m_j) to positive (m_i) ions in presence ($\chi \neq 0$) of positrons.

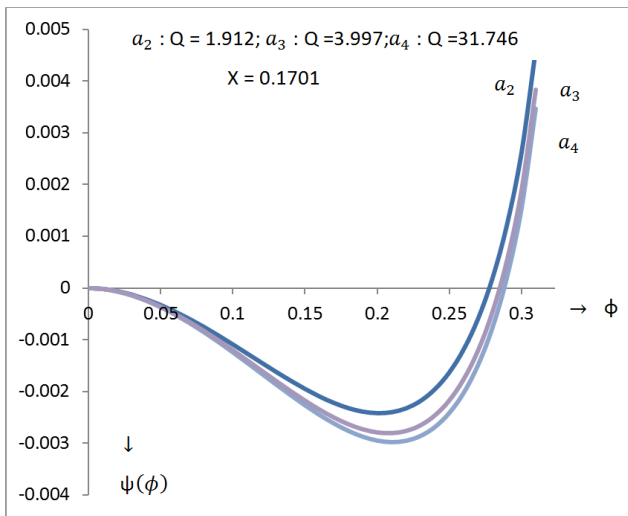


Figure 1. Profiles of Sagdeev potential function $\psi(\phi)$ against ϕ for large amplitude solitary waves in two temperature non-isothermal electron plasma under the variation of the mass ratios (Q) of negative (m_j) and positive (m_i) ions in presence of positrons for $V = 1.601$, $u_{i0} = 0.4$, $u_{j0} = 0.2$, $\sigma_i = \frac{1}{20}$, $\sigma_j = \frac{1}{25}$, $n_{j0} = 0.0501$, $n_{i0} = 0.88$, $\chi = 0.1701$, $\sigma_p = 0.4101$, $\mu = 0.15$, $\nu = 0.85$, $b_l = 0.15$, $b_h = 0.4$, $\beta_1 = 0.25$, $b_l^{(1)} = 0.24$, $b_h^{(1)} = 0.51$, $Z = 1$ when $Q = 1.912, 3.997, 31.746$.

In presence of positrons ($\chi = 0.1701$) the curves a_2 for $Q = 1.912$, a_3 for $Q = 3.997$ and a_4 for $Q = 31.746$ are shown in **Figure 1**, represent the solitary waves. The maximum value of the electrostatic potential (ϕ_m) for large amplitude solitons is increasing for increasing values of the mass ratios Q . The Sagdeev potential profiles $\psi(\phi)$ against ϕ for well shaped solitary waves denoted by a_2, a_3 and a_4 cut the ϕ axis at $\phi_m = 0.277666, 0.284871$ & 0.287948 respectively in **Figure 1**.

Figures 2, 3, 4 and 5 show the profiles of Sagdeev potential function $\psi(\phi)$ against electrostatic potential ϕ for large amplitude solitary waves under the variation of the phase velocities (V) of solitary waves in presence ($\chi \neq 0$) of positrons.

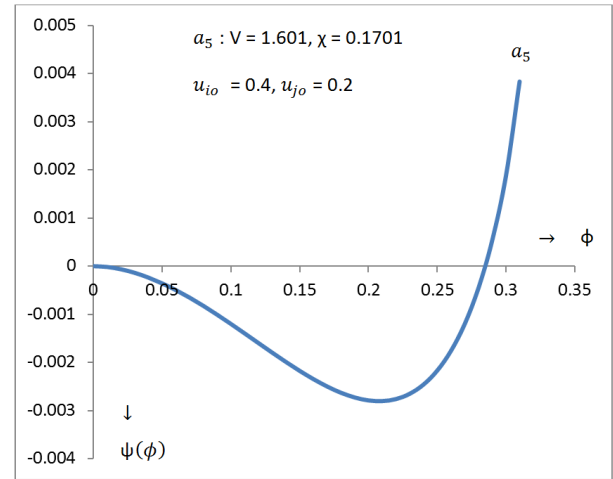


Figure 2. Profiles of Sagdeev potential function $\psi(\phi)$ against ϕ for large amplitude solitary waves in two temperature non-isothermal electron plasma under the variation of phase velocity (V) in presence of positrons for $u_{i0} = 0.4$, $u_{j0} = 0.2$, $\sigma_i = \frac{1}{20}$, $\sigma_j = \frac{1}{25}$, $n_{j0} = 0.0501$, $n_{i0} = 0.88$, $\chi = 0.1701$, $\sigma_p = 0.4101$, $\mu = 0.15$, $\nu = 0.85$, $b_l = 0.15$, $b_h = 0.4$, $\beta_1 = 0.25$, $b_l^{(1)} = 0.24$, $b_h^{(1)} = 0.51$, $Z = 1$, $Q = 3.997$ when $V = 1.601$.

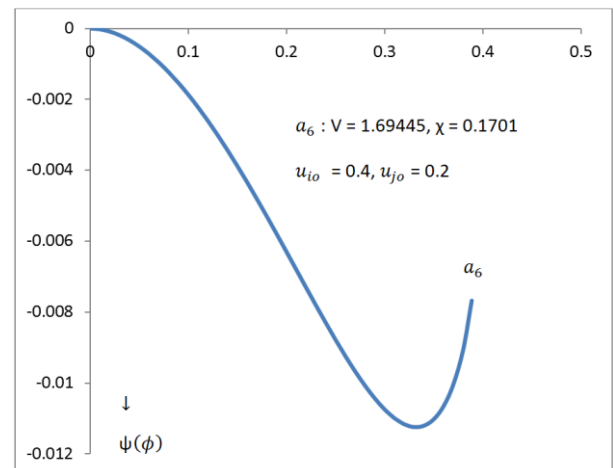


Figure 3. Profiles of Sagdeev potential function $\psi(\phi)$ against ϕ for large amplitude solitary waves in two temperature non-isothermal electron plasma under the variation of phase velocity (V) in presence of positrons for $u_{i0} = 0.4$, $u_{j0} = 0.2$, $\sigma_i = \frac{1}{20}$, $\sigma_j = \frac{1}{25}$, $n_{j0} = 0.0501$, $n_{i0} = 0.88$, $\chi = 0.1701$, $\sigma_p = 0.4101$, $\mu = 0.15$, $\nu = 0.85$, $b_l = 0.15$, $b_h = 0.4$, $\beta_1 = 0.25$, $b_l^{(1)} = 0.24$, $b_h^{(1)} = 0.51$, $Z = 1$, $Q = 3.997$ when $V = 1.69445$.

The Sagdeev potential function $\psi(\phi)$ against ϕ for large amplitude solitary waves denoted by a_5 in presence of positrons ($\chi = 0.1701$) for $V = 1.601$ with $\sigma_i = \frac{1}{20}$, $\sigma_j = \frac{1}{25}$ is shown in **Figure 2** whereas the curve a_6 in presence of positrons ($\chi = 0.1701$) for $V = 1.69445$ with $\sigma_i = \frac{1}{20}$, $\sigma_j = \frac{1}{25}$ is shown in **Figure 3**. It is seen from **Figure 3** that the curve a_6 does not show any actual well shaped solitary waves for

$V = 1.69445$ whereas the curve a_5 in Figure 2 cuts the ϕ axis at $\phi_m = 0.284871$ showing the actual well shaped soliton nature. In Figure 3, the curve a_6 does not cut the ϕ axis which shows no solitonic structure. Under this different values of V , Figures 2 and 3 present whether the well shaped nature of soliton will form or not.

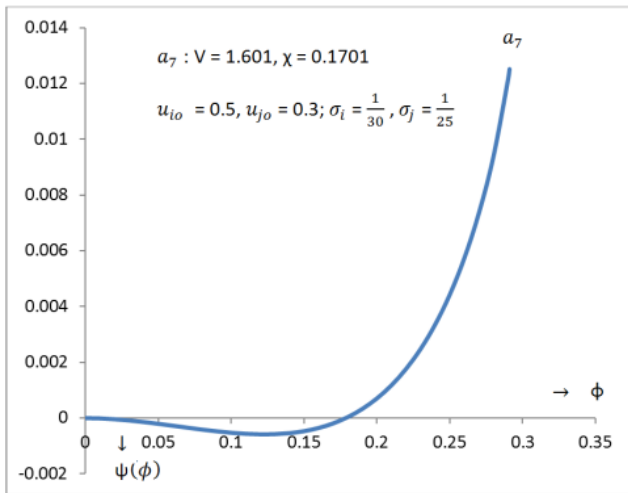


Figure 4. Profiles of Sagdeev potential function $\psi(\phi)$ against ϕ for large amplitude solitons in two temperature non-isothermal electrons under the variation of phase velocity (V) in presence of positron for $u_{i0} = 0.5, u_{j0} = 0.3, \sigma_i = \frac{1}{30}, \sigma_j = \frac{1}{25}, n_{j0} = 0.0501, n_{i0} = 0.88, \chi = 0.1701, \sigma_p = 0.4101, \mu = 0.15, \nu = 0.85, b_l = 0.15, b_h = 0.4, \beta_1 = 0.25, b_l^{(1)} = 0.24, b_h^{(1)} = 0.51, Z = 1, Q = 3.997$ when $V = 1.601$.

In Figure 4, the sagdeev potential profile $\psi(\phi)$ against electrostatic potential ϕ for large amplitude solitary waves in presence of positrons ($\chi = 0.1701$) is denoted by the curve a_7 when the temperature of positive (σ_i) and negative (σ_j) ions are $\sigma_i = \frac{1}{30}$ and $\sigma_j = \frac{1}{25}$ with $V = 1.601, u_{i0} = 0.5, u_{j0} = 0.3$. The curve a_7 cuts the ϕ axis at $\phi_m = 0.17862$ showing their soliton nature.

In Figure 5, the profile of sagdeev potential function $\psi(\phi)$ against electrostatic potential ϕ for large amplitude solitons in presence of positrons ($\chi = 0.1701$) is denoted by a_8 when the temperatures of positive (σ_i) and negative (σ_j) ions are $\sigma_i = \frac{1}{30}$ and $\sigma_j = \frac{1}{25}$ with $V = 1.69445, u_{i0} = 0.5, u_{j0} = 0.3$. In presence of positrons ($\chi = 0.1701$) the curve a_8 cuts the ϕ axis at $\phi_m = 0.342575$ showing the actual well shaped soliton nature.

Similarly it is further found that the profiles of sagdeev potential function $\psi(\phi)$ against electrostatic potential ϕ for large amplitude solitons in presence ($\chi = 0.1701$) of positrons do not form the actual well shape for any value of ϕ within the limit for the solitary wave condition when the temperature of positive (σ_i) and negative (σ_j) ions are $\sigma_i = \frac{1}{25}$ and $\sigma_j = \frac{1}{20}$ with $V = 1.701, 1.801, 1.901 \& 1.99631, u_{i0} = 0.4, u_{j0} = 0.2, \chi = 0.1701, \sigma_p = 0.4101$.

Figure 6 represents the Sagdeev potential profiles $\psi(\phi)$ against electrostatic potential ϕ for large amplitude solitary waves under the variation of the concentrations of negative ions (n_{j0}) in presence ($\chi \neq 0$) of positrons.

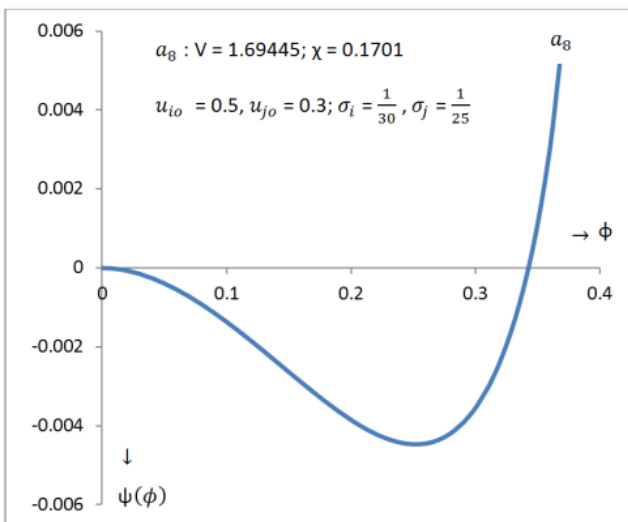


Figure 5. Profiles of Sagdeev potential function $\psi(\phi)$ against ϕ for large amplitude solitary waves in two temperature non-isothermal electron plasma under the variation of phase velocity (V) in presence of positrons for $u_{i0} = 0.5, u_{j0} = 0.3, \sigma_i = \frac{1}{30}, \sigma_j = \frac{1}{25}, n_{j0} = 0.0501, n_{i0} = 0.88, \chi = 0.1701, \sigma_p = 0.4101, \mu = 0.15, \nu = 0.85, b_l = 0.15, b_h = 0.4, \beta_1 = 0.25, b_l^{(1)} = 0.24, b_h^{(1)} = 0.51, Z = 1, Q = 3.997$ when $V = 1.69445$.

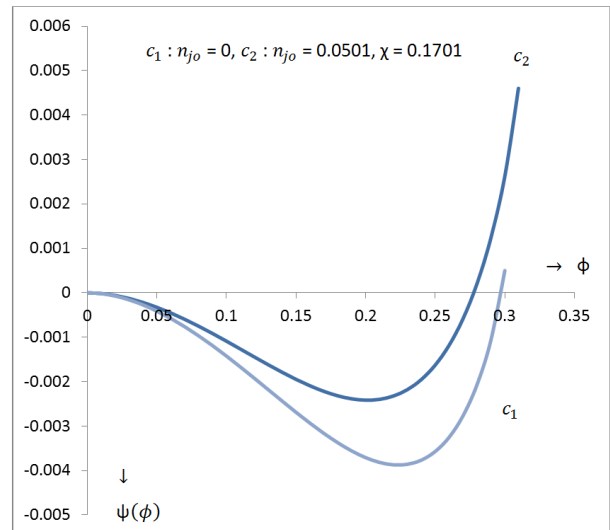


Figure 6. Profiles of Sagdeev potential function $\psi(\phi)$ against ϕ for large amplitude solitary waves in two temperature non-isothermal electron plasma under the variation of the negative ion concentrations (n_{j0}) in presence of positrons for $u_{i0} = 0.4, u_{j0} = 0.2, \sigma_i = \frac{1}{20}, \sigma_j = \frac{1}{25}, \chi = 0.1701, \sigma_p = 0.4101, \mu = 0.15, \nu = 0.85, b_l = 0.15, b_h = 0.4, \beta_1 = 0.25, b_l^{(1)} = 0.24, b_h^{(1)} = 0.51, Z = 1, Q = 1.912, V = 1.601, n_{i0} = 0.8299, 0.88$ when $n_{j0} = 0, 0.0501$.

In presence of positrons ($\chi = 0.1701$), the sagdeev potential profiles $\psi(\phi)$ against the electrostatic potential ϕ for large amplitude solitary waves are denoted by c_1 for $n_{j_0} = 0$ and c_2 for $n_{j_0} = 0.0501$ when $V = 1.601, u_{i_0} = 0.4, u_{j_0} = 0.2, \sigma_i = \frac{1}{20}, \sigma_j = \frac{1}{25}$. The curves c_1 and c_2 cut the ϕ axis at $\phi_m = 0.297416$ and $\phi_m = 0.277660$ respectively showing their well shaped soliton nature. This shows the effect of concentrations of negative ions on Sagdeev potential function $\psi(\phi)$ in presence of positrons.

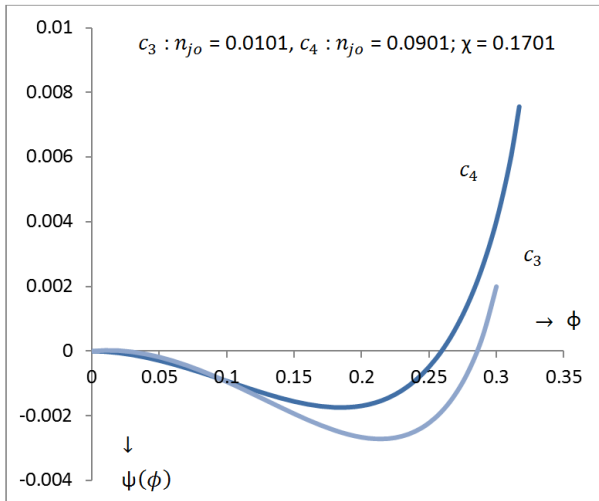


Figure 7. Profiles of Sagdeev potential function $\psi(\phi)$ against ϕ for large amplitude solitary waves in two temperature non-isothermal electron plasma under the variation of the concentrations (n_{j_0}) in presence of positrons for $u_{i_0} = 0.4, u_{j_0} = 0.2, \sigma_i = \frac{1}{20}, \sigma_j = \frac{1}{25}, \chi = 0.1701, \sigma_p = 0.4101, \mu = 0.15, \nu = 0.85, b_l = 0.15, b_h = 0.4, \beta_1 = 0.25, b_l^{(1)} = 0.24, b_h^{(1)} = 0.51, Z = 1, Q = 1.912, V = 1.601, n_{i_0} = 0.84, 0.9$ when $n_{j_0} = 0.0101, 0.0901$.

In Figure 7, the sagdeev potential function $\psi(\phi)$ against the electrostatic potential ϕ for large amplitude solitary waves in presence ($\chi = 0.1701$) of positrons are denoted by c_3 for $n_{j_0} = 0.0101$ and c_4 for $n_{j_0} = 0.0901$ when $V = 1.601, u_{i_0} = 0.4, u_{j_0} = 0.2, \sigma_i = \frac{1}{20}, \sigma_j = \frac{1}{25}$. It is evident from this figure that the curve c_3 for $n_{j_0} = 0.0101$ cuts the ϕ axis at a larger distance than the curve c_4 for $n_{j_0} = 0.0901$ with $\chi = 0.1701$ where the curve c_4 cuts the ϕ axis at $\phi_m = 0.259325$. The Figures 6 and 7 show the characteristics of the sagdeev potential function under the variation of the concentration of negative ions (n_{j_0}) in presence ($\chi = 0.1701$) of positrons.

In Figure 8, the profiles of Sagdeev potential function $\psi(\phi)$ against the electrostatic potential ϕ for large amplitude solitary waves are drawn under the variation of the concentrations of positrons (χ). For different values of the concentrations of positrons (χ), the sagdeev potential function $\psi(\phi)$ cuts the ϕ axis at different values. The sagdeev potential function $\psi(\phi)$ at $\chi = 0.0801$ denoted by c_5 cuts the ϕ axis

at $\phi_m = 0.213413$ and at $\chi = 0.1201$, the sagdeev potential function $\psi(\phi)$ denoted by c_6 cuts the ϕ axis at $\phi_m = 0.246681$. The curve c_7 represents the sagdeev potential function $\psi(\phi)$ cuts the ϕ axis at $\phi_m = 0.277660$ for $\chi = 0.1701$ which is larger than all other values.

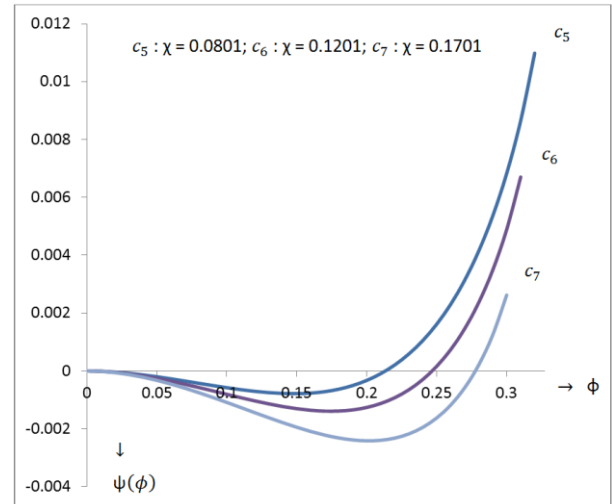


Figure 8. Profiles of Sagdeev potential function $\psi(\phi)$ against ϕ for large amplitude solitary waves in two temperature non-isothermal electron plasma under the variation of the concentrations (χ) of positrons for $V = 1.601, u_{i_0} = 0.4, u_{j_0} = 0.2, \sigma_i = \frac{1}{20}, \sigma_j = \frac{1}{25}, n_{j_0} = 0.0501, n_{i_0} = 1.0501, 0.97, 0.93, 0.88, \sigma_p = 0, 0.4101, \mu = 0.15, \nu = 0.85, b_l = 0.15, b_h = 0.4, \beta_1 = 0.25, b_l^{(1)} = 0.24, b_h^{(1)} = 0.51, Z = 1, Q = 1.912$ when $\chi = 0.0801, 0.1201, 0.1701$.

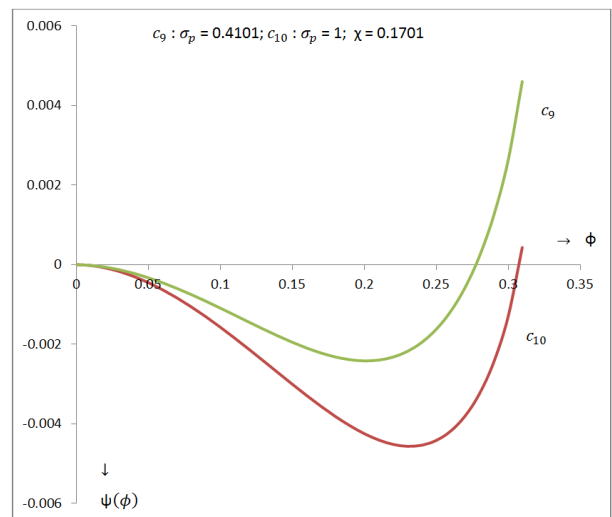


Figure 9. Profiles of Sagdeev potential function $\psi(\phi)$ against ϕ for large amplitude solitons in two temperature non-isothermal electrons under the variation of the temperature ratios (σ_p) of electrons and positrons for $V = 1.601, u_{i_0} = 0.4, u_{j_0} = 0.2, \sigma_i = \frac{1}{20}, \sigma_j = \frac{1}{25}, n_{j_0} = 0.0501, n_{i_0} = 0.88, \chi = 0.1701, \mu = 0.15, \nu = 0.85, b_l = 0.15, b_h = 0.4, \beta_1 = 0.25, b_l^{(1)} = 0.24, b_h^{(1)} = 0.51, Z = 1, Q = 1.912$ when $\sigma_p = 0.4101, 1$.

In Figure 9, the Sagdeev potential profiles $\psi(\phi)$ against the electrostatic potential ϕ for large amplitude solitons are drawn under the variation of the different temperature ratios (σ_p) of electron (T_e) and positron (T_p). It is observed from Figures 9 and 10 that the Sagdeev potential profiles cut the ϕ axis at larger distances as long as the temperature ratios (σ_p) of electron (T_e) and positron (T_p) is increasing. The Sagdeev potential profiles $\psi(\phi)$ against ϕ for solitary waves are denoted respectively by the curves c_9 for $\sigma_p = 0.4101$, c_{10} for $\sigma_p = 1$ in Figure 9 and c_{12} for $\sigma_p = 1.301$, c_{13} for $\sigma_p = 1.9501$ in Figure 10. In Figure 9, the Sagdeev potential curves for actual well shaped solitary waves denoted by c_9 for $\sigma_p = 0.4101$ cuts the ϕ axis at $\phi_m = 0.277660$, c_{10} for $\sigma_p = 1$ cuts the ϕ axis at $\phi_m = 0.307871$ but in Figure 10, for $\sigma_p = 1.301$ and 1.9501 no solitary waves for actual well shaped are found and thus it is concluded that for $\sigma_p > 1$ no proper solitary waves are found in two-temperature non-isothermal electron plasmas in presence of negative ions.

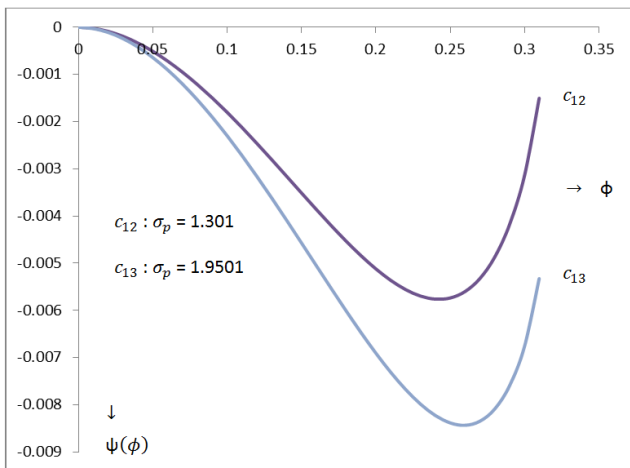


Figure 10. Profiles of Sagdeev potential function $\psi(\phi)$ against ϕ for large amplitude solitons in two temperature non-isothermal electrons under the variation of the temperature ratios of electrons and positrons (σ_p) for $V = 1.601$, $u_{i0} = 0.4$, $u_{j0} = 0.2$, $\sigma_i = \frac{1}{20}$, $\sigma_j = \frac{1}{25}$, $n_{j0} = 0.0501$, $n_{i0} = 0.88$, $\chi = 0.1701$, $\mu = 0.15$, $v = 0.85$, $b_l = 0.15$, $b_h = 0.4$, $\beta_1 = 0.25$, $b_l^{(1)} = 0.24$, $b_h^{(1)} = 0.51$, $Z = 1$, $Q = 1.912$ when $\sigma_p = 1.301, 1.9501$.

In the next part, we are now presenting graphically the profiles of small amplitude double layers in presence ($\chi = 0.1701$) of positrons under the variation of some plasma parameters.

In Figure 11, the profiles of Sagdeev potential function $\psi(\phi)$ against the electrostatic potential ϕ for small amplitude double layers are drawn in presence ($\chi = 0.1701$) of positrons under the variation of the phase velocity (V) of solitary waves. In presence of positrons ($\chi = 0.1701$), the

Sagdeev potential profiles $\psi(\phi)$ against ϕ for small amplitude double layers are denoted by p_1 for $V = 1.6501$, p_2 for $V = 1.6801$. It is evident from the figure that for increasing values of V , the maximum values of the electrostatic potential (ϕ_{dl}) where the respective curves cut the ϕ axis are larger.

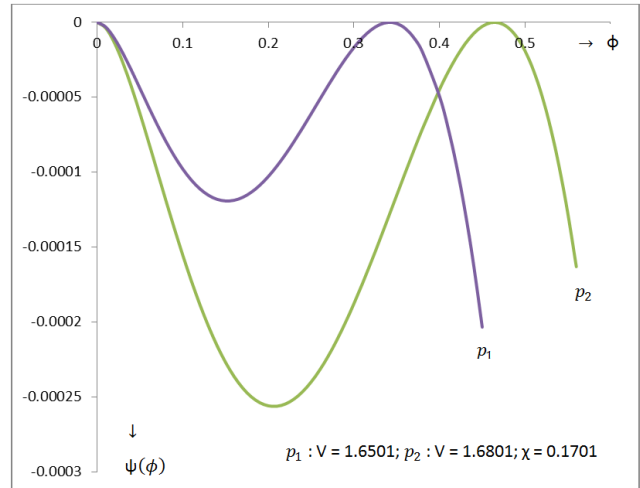


Figure 11. Profile of Sagdeev potential function $\psi(\phi)$ against ϕ for small amplitude double layers in presence of positrons under the variation of phase velocity (V) of solitary waves for $u_{i0} = 0.4$, $u_{j0} = 0.2$, $\sigma_i = \frac{1}{25}$, $\sigma_j = \frac{1}{20}$, $n_{j0} = 0.0501$, $n_{i0} = 0.88$, $\chi = 0.1701$, $\sigma_p = 0.4101$, $\mu = 0.15$, $v = 0.85$, $b_l = 0.15$, $b_h = 0.4$, $\beta_1 = 0.25$, $b_l^{(1)} = 0.24$, $b_h^{(1)} = 0.51$, $Z = 1$, $Q = 1.912$ when $V = 1.6501, V = 1.6801$.

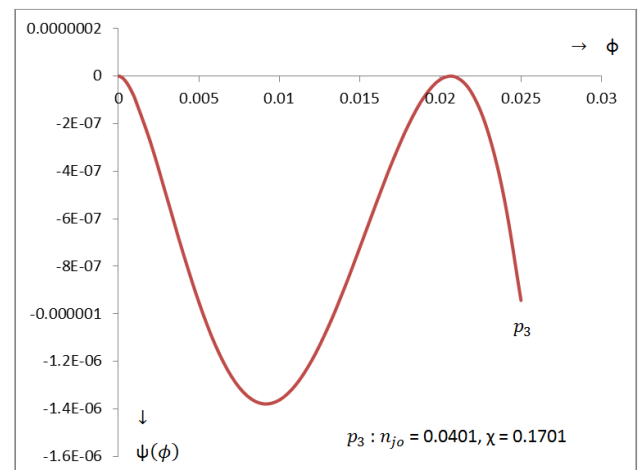


Figure 12. Profile of Sagdeev potential function $\psi(\phi)$ against ϕ for small amplitude double layers in presence of positrons under the variation of the concentration of negative ions (n_{j0}) for $V = 1.6501$, $u_{i0} = 0.4$, $u_{j0} = 0.2$, $\sigma_i = \frac{1}{25}$, $\sigma_j = \frac{1}{20}$, $\chi = 0.1701$, $\sigma_p = 0.4101$, $\mu = 0.15$, $v = 0.85$, $b_l = 0.15$, $b_h = 0.4$, $\beta_1 = 0.25$, $b_l^{(1)} = 0.24$, $b_h^{(1)} = 0.51$, $Z = 1$, $Q = 1.912$, $n_{i0} = 0.87$ when $n_{j0} = 0.0401$.

Figures 12 and 13 show the profiles of Sagdeev potential function $\psi(\phi)$ against the electrostatic potential ϕ for small amplitude double layers in presence of positrons ($\chi = 0.1701$) under the variation of the concentrations of negative ions (n_{jo}). In Figure 12, when the concentration of negative ions is $n_{jo} = 0.0401$, the Sagdeev potential profile $\psi(\phi)$ against ϕ for small amplitude double layers is represented by the curve p_3 for $\chi = 0.1701$ whereas in Figure 13, when the concentration of negative ions is $n_{jo} = 0.0501$, the Sagdeev potential profile $\psi(\phi)$ against ϕ for small amplitude double layers is denoted by the curve p_4 for $\chi = 0.1701$. In Figure 12, it is observed that the curve p_3 in presence of positron ($\chi = 0.1701$) cuts the ϕ axis at $\phi_{dl} = 0.020621$ while in Figure 13, the Sagdeev potential profile $\psi(\phi)$ against ϕ for small amplitude double layers denoted by the curve p_4 for $\chi = 0.1701$ cuts the ϕ axis at $\phi_{dl} = 0.342005$ when the concentration of negative ions is $n_{jo} = 0.0501$.

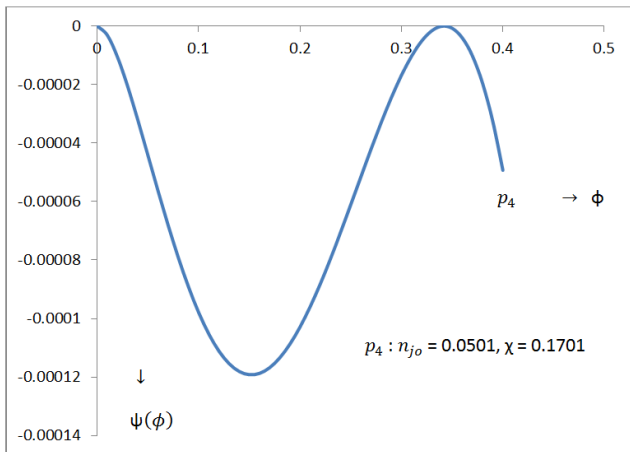


Figure 13. Profile of Sagdeev potential function $\psi(\phi)$ against ϕ for small amplitude double layers in presence of positrons under the variation of the concentration of negative ions (n_{jo}) for $V = 1.6501$, $u_{io} = 0.4$, $u_{jo} = 0.2$, $\sigma_i = \frac{1}{25}$, $\sigma_j = \frac{1}{20}$, $\chi = 0.1701$, $\sigma_p = 0.4101$, $\mu = 0.15$, $\nu = 0.85$, $b_l = 0.15$, $b_h = 0.4$, $\beta_1 = 0.25$, $b_l^{(1)} = 0.24$, $b_h^{(1)} = 0.51$, $Z = 1$, $Q = 1.912$, $n_{io} = 0.88$ when $n_{jo} = 0.0501$.

Figure 14 shows the profiles of Sagdeev potential function $\psi(\phi)$ against the electrostatic potential ϕ for small amplitude double layers under the variation of the temperature ratios (σ_p) of electrons (T_e) and positrons (T_p). The Sagdeev potential profiles $\psi(\phi)$ against ϕ for small amplitude double layers in presence of positron ($\chi = 0.1701$) denoted by p_6 for $\sigma_p = 0.1501$ and p_7 for $\sigma_p = 0.4101$ cut the ϕ axis at $\phi_{dl} = 0.322136$ and 0.342005 respectively. In this case, it is found that as σ_p increases ϕ_{dl} also increases.

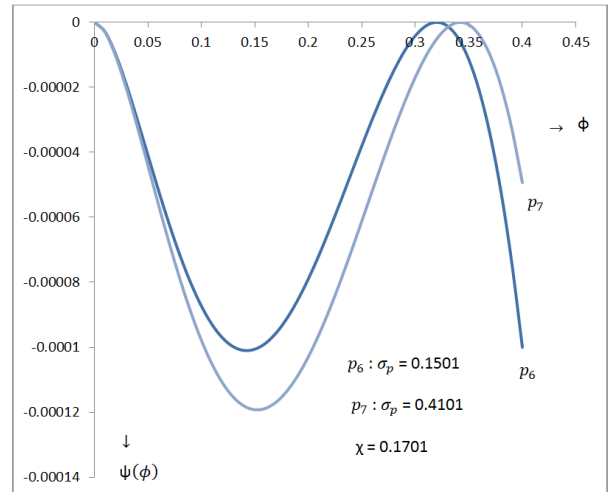


Figure 14. Profiles of Sagdeev potential function $\psi(\phi)$ against ϕ for small amplitude double layers in presence of positrons under the variation of the temperature ratios (σ_p) of electrons and positrons for $V = 1.6501$, $u_{io} = 0.4$, $u_{jo} = 0.2$, $\sigma_i = \frac{1}{25}$, $\sigma_j = \frac{1}{20}$, $n_{jo} = 0.0501$, $n_{io} = 0.88$, $\chi = 0.1701$, $\mu = 0.15$, $\nu = 0.85$, $b_l = 0.15$, $b_h = 0.4$, $\beta_1 = 0.25$, $b_l^{(1)} = 0.24$, $b_h^{(1)} = 0.51$, $Z = 1$, $Q = 1.912$ when $\sigma_p = 0.1501, 0.4101$.

From Figure 14, it is observed that in presence of positron ($\chi = 0.17$), the Sagdeev potential profiles $\psi(\phi)$ against ϕ for small amplitude double layers cut the ϕ axis at larger values of ϕ_{dl} for higher values of σ_p while for the smaller values of σ_p the respective Sagdeev potential curves for small amplitude double layers cut the ϕ axis at smaller values of ϕ_{dl} .

4. Conclusion

In this paper, the present author investigated the large amplitude ion-acoustic compressive solitary waves and small amplitude ion-acoustic compressive double layers in two-temperature non-isothermal electron plasmas consisting of warm negative ions, warm positive ions and warm positrons by Sagdeev pseudopotential method under the variation of different plasma parameters. In presence ($\chi \neq 0$) of positrons, the nature of Sagdeev potential function $\psi(\phi)$ for large amplitude ion-acoustic compressive solitary waves are shown in Figures 1 to 10 under the variation of the mass ratios (Q) of negative to positive ions, phase velocities (V) of solitary waves, concentrations (n_{jo}) of negative ions, concentrations of positrons (χ) and temperature ratios (σ_p) of electrons (T_e) and positrons (T_p). In Figures 11 to 14, the profiles of Sagdeev potential profiles $\psi(\phi)$ against electrostatic potential ϕ for small amplitude double layers are presented graphically under the variation of the phase velocity (V) of solitary waves, concentration of negative ions (n_{jo}) and temperature ratios (σ_p) of electrons (T_e) and positrons (T_p). In presence of positrons, the

author studied and discussed the effect of positrons for large amplitude solitons and small amplitude double layers. Generally solitons are important in understanding energy transport in space plasmas and have been considered in plasma-based devices for signal transmission without dissipation. On the other hand, double layers are relevant in the context of space weather phenomena and are important for understanding energy dissipation and particle acceleration mechanisms in astrophysical plasmas. The present study has been used in the experimental investigation of strong double layers for $(\text{Ar}^+, \text{SF}_6^-)$ plasma and will be helpful for the investigation of ion-acoustic waves in space and in laboratory experiments.

The author's future plan is to solve the fully non-linear differential equations for relativistic warm positive and negative ions, two-temperature isothermal electrons and warm isothermal positrons to investigate the ion-acoustic compressive (rarefactive) solitary waves, double layers and supersolitons.

Abbreviations

SPM Sagdeev Pseudopotential Method

Acknowledgments

The present author would like to thank Dr. S.N. Paul for his valuable suggestions and discussions in the preparation of this paper to its present form.

Funding

Thus this research work did not receive any specific grant from any funding agencies in the public, commercial, or not-for-profit sectors.

Conflicts of Interest

The author declares no conflicts of interest.

References

- [1] M. K. Kalita and S. Bujarbarua, *Can. J. Phys.* 60, (1982) 392 - 396. <https://doi.org/10.1139/p82-057>
- [2] S. G. Tagare and R. V. Reddy, *J. Plasma Phys.* 35, (1986) 219. <https://doi.org/10.1017/S0022377800011296>
- [3] S. G. Tagare and R. V. Reddy, *Plasma Phys. and Controlled Fusion*, 29(6), (1987) 671 - 676. <https://doi.org/10.1088/0741-3335/29/5/008>
- [4] S. Chattopadhyay, *Brazilian Journal of Physics*, 52(4), (2022) 117. <https://doi.org/10.1007/s13538-022-01120-9>
- [5] R. V. Reddy and S. G. Tagare, *J. Physical Soc. Japan*, 56(12), (1987) 4329 - 4335 <https://doi.org/10.1143/JPSJ.56.4329>
- [6] S. Chattopadhyay and S. N. Paul, *The African Review of Phys.* 7:0033, (2012) 289 - 299.
- [7] K. P. Das, S. R. Majumdar and S. N. Paul, *Phys. Rev. E* 51, (1995) 4796. <https://doi.org/10.1103/PhysRevE51.4796>
- [8] S. Chattopadhyay, *The African Review of Phys.* 9: 0041, (2014) 317 - 331.
- [9] B. N. Goswami and B. Buti, *Phys. Letts. A*, 57,2, (1976) 149 - 150. [https://doi.org/10.1016/0375-9601\(76\)90195-X](https://doi.org/10.1016/0375-9601(76)90195-X)
- [10] S. Chattopadhyay, *Sri Lankan Journal of Phys.* 29, (2019) 1 - 16. <https://doi.org/10.4038/SIjp.v20i0.8062>
- [11] T. S. Gill, P. Bala, H. Kaur, N. S. Saini, S. Bansal and J. Kaur, *The Euro. Phys. J. D* 31, (2004) 91. <https://doi.org/10.1140/epjd/e2004-00121-4>
- [12] M. Tajiri and M. Tuda, *J. Phys. Soc. Jpn.* 54, (1985) 19. <https://doi.org/10.1143/JPSJ.54.19>
- [13] G. C. Das, B. Karmakar and S. N. Paul, *IEEE Trans. Plasma Sci.* 16(1), (1988) 22 - 26. <https://doi.org/10.1109/27.3785>
- [14] M. K. Mishra, R. S. Chhabra and S. R. Sharma, *J. Plasma Phys.* 52(3), (1994) 409 - 429. <https://doi.org/10.1017/S0022377800027227>
- [15] S. Chakraborty, A. Roychowdhury and S. N. Paul, *Inter. J. Theor. Phys.* 32, (1993) 1465. <https://doi.org/10.1007/BF00675208>
- [16] S. G. Tagare, *Phys. Plasmas*, 7(3) (2000) 883 - 888. <https://doi.org/10.1063/1.873885>
- [17] A. Y. Wong, D. L. Mamas and D. Arnush, *Phys. Fluids* 18(11) (1975) 1489 - 1493. <https://doi.org/10.1063/1.861034>
- [18] S. Chattopadhyay, *Sri Lankan Journal of Phys.* 23(2), (2022) 93 - 124. <https://doi.org/10.4038/SIjp.v23i2.8090>
- [19] S. Chattopadhyay, *Jurnal Fizik Malaysia* 43(1), (2022) 10214 - 10243.
- [20] S. Chattopadhyay, *Brazzilian Journal of Phys.* 53, (2023) 6. <https://doi.org/10.1007/s13538-022-01205-5>
- [21] G. C. Das, S. G. Tagare and J. Sarma, *Planet Space Sci.* 46(4), (1998) 417 - 424. [https://doi.org/10.1016/S0032-0633\(97\)00142-6](https://doi.org/10.1016/S0032-0633(97)00142-6)
- [22] R. Roychowdhury, G. C. Das and J. Sharma, *Phys. Plasma* 6(7), (1999) 2721 - 2726. <https://doi.org/10.1063/1.873228>
- [23] K. S. Goswami and S. Bujarbarua, *Phys. Lett. A*, 108(3), (1985) 149 - 152. [https://doi.org/10.1016/0375-9601\(85\)90847-3](https://doi.org/10.1016/0375-9601(85)90847-3)
- [24] R. Bharuthram and P. K. Shukla, *Phys. Fluids* 29, (1986) 3214. <https://doi.org/10.1063/1.865839>
- [25] L. L. Yadav and S. R. Sharma, *Phys. Scr.* 43(1), (1991) 106. <https://doi.org/10.1088/0031-8949/43/1/018>
- [26] A. N. Sekar and Y. C. Saxena, *Plasma Phys. Controlled Fusion* 27(2), (1985) 181. <https://doi.org/10.1088/0741-3335/27/2/007>

- [27] N. Hershkowitz, *Space Sci. Rev.* 41, (1985) 351 – 391. <https://doi.org/10.1007/BF00190655>
- [28] G. Hairapetian and R. L. Stenzel, *Phys. Rev. Lett.* 65, (1990) 175. <https://doi.org/10.1103/PhysRevLett.65.175>
- [29] G. C. Das and S. G. Tagare, *Plasma Phys.* 17(12), (1975) 1025. <https://doi.org/10.1088/0032-1028/17/12/002>
- [30] S. Watanabe, *J. Phy. Soc. Japan* 53(3), (1984) 950 – 956. <https://doi.org/10.1143/JPSJ.53.950>
- [31] S. G. Tagare, *J. Plasma Phys.* 36, (1986) 301. <https://doi.org/10.1017/S0022377800011776>
- [32] J. L. Cooney, M. T. Gavin and K. E. Lonngren, *Phys. Fluids B* 10, (1991) 2758 – 2766. <https://doi.org/10.1063/1.859912>
- [33] M. K. Mishra, A. K. Arora and R. S. Chhabra, *Phys. Rev. E* 66, (2002) 046402. <https://doi.org/10.1103/PhysRevE.66.046402>
- [34] R. L. Merlino and J. J. Loomis, *Phys. Fluids B* 2, (1990) 2865 – 2867. <https://doi.org/10.1063/1.859355>
- [35] S. Chattopadhyay, S. K. Bhattacharaya and S. N. Paul, *Indian J. Phys.* 76 B (1), (2002) 59 – 65.
- [36] S. Chattopadhyay, S. N. Paul and D. Ray, *Fizika A (Zagreb)* 18, 3, (2009) 89 – 106.
- [37] R. Z. Sagdeev, *Reviews of Plasma Physics*, Consultants Bureau, New York, 4, (1966) 23.
- [38] K. K. Ghosh, D. Ray and S. N. Paul, *Int. J. Theoretical Phys.* 31(1), (1992) 75 – 80. <http://doi.org/10.1007/BF00674342>
- [39] G. C. Das and A. Nag, *Assam Univ. J. Sci. Technol.* 5, (2010) 169.
- [40] M. Temerin, K. Cerny, W. Lotko and F. S. Mozer, *Phys. Rev. Lett.* 48, (1982) 1175. <https://doi.org/10.1103/PhysRevLett.48.1175>
- [41] R. Bostrom, G. Gustafsson, B. Holback, G. Holmgren, H. Koskinen and P. Kintner, *Phys. Rev. Lett.* 61, (1988) 82. <https://doi.org/10.1103/PhysRevLett.61.82>
- [42] S. I. Popel, S. V. Vladimirov and P. K. Shukla, *Phys. Plasmas* 2, (1995) 716 – 719. <https://doi.org/10.1063/1.871422>